

Molecular Physics

An International Journal at the Interface Between Chemistry and Physics

ISSN: 0026-8976 (Print) 1362-3028 (Online) Journal homepage: www.tandfonline.com/journals/tmph20

Lamb-dip spectroscopy of HD at cryogenic temperatures down to 12 K

Q.-H. Liu, Y.-N. Lv, C.-F. Cheng & S.-M. Hu

To cite this article: Q.-H. Liu, Y.-N. Lv, C.-F. Cheng & S.-M. Hu (09 Mar 2026): Lamb-dip spectroscopy of HD at cryogenic temperatures down to 12 K, Molecular Physics, DOI: [10.1080/00268976.2026.2641679](https://doi.org/10.1080/00268976.2026.2641679)

To link to this article: <https://doi.org/10.1080/00268976.2026.2641679>



Published online: 09 Mar 2026.



Submit your article to this journal [↗](#)



View related articles [↗](#)



View Crossmark data [↗](#)

Lamb-dip spectroscopy of HD at cryogenic temperatures down to 12 K

Q.-H. Liu^a, Y.-N. Lv^{a,b}, C.-F. Cheng^{b,a,c} and S.-M. Hu^{b,a,c}

^aHefei National Research Center for Physical Sciences at Microscale, University of Science and Technology China, Hefei, People's Republic of China; ^bCAS Center for Excellence in Quantum Information and Quantum Physics, University of Science and Technology of China, Hefei, People's Republic of China; ^cHefei National Laboratory, University of Science and Technology China, Hefei, People's Republic of China

ABSTRACT

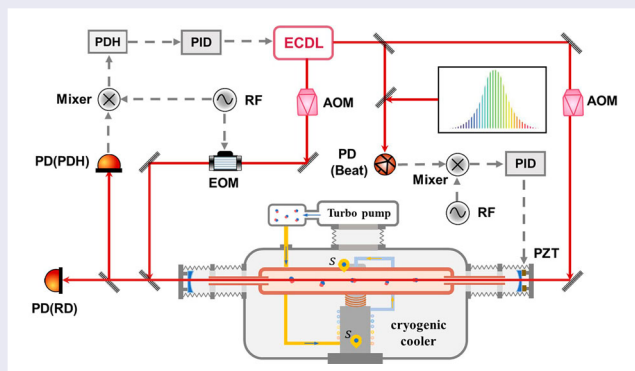
Precision measurements of molecular hydrogen and its isotopologues provide critical tests of molecular theory, including quantum electrodynamics (QED) and fundamental constants. However, advancing the experimental accuracy of hydrogen overtone transitions remains challenging due to unexplained asymmetries in spectral line profiles. We present the Lamb dip measurement at a temperature as low as 12 K, where the spectral features exhibit enhanced resolution. By applying a lineshape centroid extrapolation method – which is independent of the lineshape model – we determine the transition frequency of the R(0) line in the (2-0) overtone of HD to be 214 905 335 170 (27)_{stat}(124)_{sys} kHz. While the low-temperature Lamb-dip measurements challenge conventional models of spectral line shapes, our results are in excellent agreement with the latest theoretical results.

ARTICLE HISTORY

Received 15 December 2025
Accepted 1 March 2026

KEYWORDS

Molecular hydrogen;
cryogenic temperature;
cavity-enhanced
spectroscopy



1. Introduction

The hydrogen molecule and its isotopologues represent the simplest two-electron molecules, making them ideal for precise spectroscopic measurements and rigorous tests of quantum theory. By combining high-accuracy experimental data with first-principle calculations, including relativistic and quantum electrodynamics (QED) corrections, these molecules serve as benchmarks for validating quantum mechanics and determining fundamental physical constants such as the proton-electron mass ratio [1–5]. For nearly a century, extensive efforts have focussed on measuring the dissociation energy of the hydrogen molecule, D_0 (H_2), achieving agreement between theory and experiment at the 10-digit level [6–8].

The most accurate previous determination of D_0 (H_2) involved two-photon Doppler-free laser excitation to the EF $^1\Sigma_g^+$ ($\nu = 0, N = 1$) intermediate state using the Ramsey comb method [9], one-photon ultraviolet excitation from the EF $^1\Sigma_g^+$ (0,1) state to the 54p1₁ Rydberg state [10], and millimetre wave (MMW) spectroscopy of high-lying Rydberg states, extrapolated to the ionisation energy by Multi-Channel Quantum Defect theory (MQDT) [11]. However, this approach is limited by the short lifetime of the intermediate electronic state, which introduces uncertainties due to natural linewidth. In contrast, rovibrational transitions, owing to their narrow natural linewidth, enable measurements with unprecedented precision. The heteronuclear isotopologue of molecular hydrogen, HD, exhibits stronger rovibrational

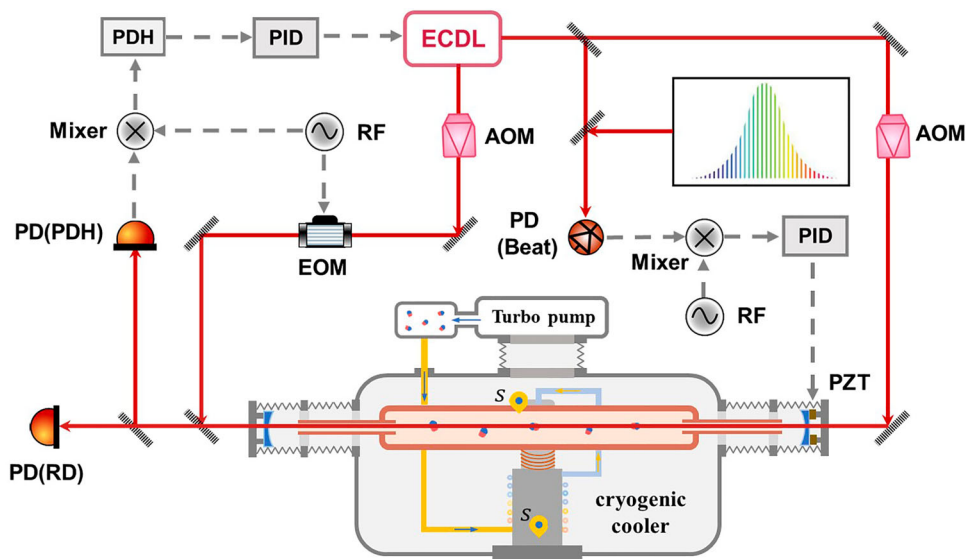


Figure 1. The experimental apparatus. The blue colour indicates the ring-down cavity mirrors. The orange indicates the sample cell made of Oxygen-Free High-Conductivity (OFHC) copper. The grey colour refers to the vacuum chamber, and the inner wall of the chamber is electrolytically polished. AOM: acousto-optical modulator; EOM: electro-optical modulator; RF: Radio Frequency; S: temperature sensor; PD(PDH): detector for PDH locking; PD(RD): detector for ring-down events. PD(Beat): detector for laser beating.

transitions compared to H_2 or D_2 , owing to its non-zero electric dipole moment. H_2 and D_2 possess only quadrupole transitions in the electronic ground state. Various spectroscopy techniques have been employed to determine rovibrational energies of HD, including direct absorption in gas cell for fundamental and overtone transitions [12–14], Doppler-free cavity-enhanced spectroscopy for the R(1) and P(1) of the (2-0) overtone band [5,15–18], and Resonance-Enhanced Multiphoton Ionisation (REMPI) spectroscopy in molecular beam for the R(0) line in the fundamental band [19]. The REMPI measurement currently holds the record for precision, achieving an uncertainty of 13 kHz for the R(0) (1-0) line of HD [19].

Despite these advances, Doppler-free spectroscopy of HD faces a critical challenge: asymmetric line shapes that hinder further improvements in accuracy. Both the Amsterdam and Hefei groups have observed this phenomenon [16,18], but their interpretations differ. The Hefei group attributes the asymmetry to coupling between far-detuned strong electronic transitions and the standing wave light field [20], proposing a systematic correction to account for the distortion [21]. While the Amsterdam group suggests that intermolecular interactions, combined with hyperfine structure, are responsible for this asymmetry. They emphasise that the complex hyperfine energy level structure complicates spectral analysis and have consequently shifted their focus to Lamb-dip spectroscopy of other isotopologues with simpler hyperfine structures [22]. This discrepancy underscores the need for further high-precision measurements of HD

rovibrational transitions, particularly at lower temperatures where spectral resolution can be improved.

In the present work, we report saturated absorption spectroscopy of the R(0) line in the (2-0) overtone band of HD, with the molecular sample cooled to 12 K. This ultralow-temperature approach significantly enhances spectral resolution, revealing unusual Lamb-dip profiles. Our results provide new insights into the mechanisms underlying line-shape asymmetry and pave the way for future precision measurements.

2. Experiment

The experimental setup for measuring saturated absorption spectra of HD is schematically shown in Figure 1, based on a comb-locked cavity ring-down spectroscopy (CRDS) instrument adapted from our previous studies [5,21]. The CRDS technique determines the decay time constant τ of light transmitted from an optical cavity after the input light is shut off. The absorption coefficient of the sample can be directly obtained from the difference in $(c\tau)^{-1}$, where c is the speed of light. This method was employed in our study due to its high sensitivity and the fact that it requires no additional modulation-demodulation processes. An external cavity diode laser (ECDL) operating at 1395 nm with approximately 60 mW output power was split into three branches for different functions. One of the laser beams, with s-polarization, underwent a -160 MHz frequency shift through a double-pass acousto-optic modulator (AOM) configuration and served as the locking beam stabilised

to the ring-down cavity using the Pound-Drever-Hall (PDH) method. The high-finesse cavity, formed by mirrors with a reflectivity of $R \approx 99.997\%$ and a radius of curvature $\rho \approx 1$ m, has a cavity finesse of $\sim 1.1 \times 10^5$ and a free spectra range of about 240 MHz. One of the cavity mirrors was attached to a piezo actuator for precise cavity length adjustment and optical mode frequency control. A second beam, with p-polarisation, received a +80 MHz frequency shift and delivered the primary optical power for ring-down measurements. The low-loss mirrors enabled intra-cavity power levels up to 220 W. The circular laser power inside the cavity could be estimated [23] from the transmitted laser power and the mirror transmittance. The third beam provided metrological reference through heterodyne detection with an optical frequency comb (OFC). The resulting error signal was compared with a preset radiofrequency (RF) reference and subsequently fed back to the cavity piezoelement. Operating at a bandwidth of approximately 1 Hz, this feedback system ensured long-term frequency stability consistent with the OFC performance. A direct digital synthesiser (DDS) generated the RF reference signal, thereby enabling precise frequency scanning for spectral acquisition. All frequency generation and measurement devices were phase-locked to a GPS-disciplined Rb clock, ensuring relative frequency accuracy better than 1×10^{-13} throughout the experiments.

The saturation intensity [24] of the R(0) transition of HD is very high: $I_{sat} = \frac{ch}{3} \frac{\gamma^2 k^3}{A} \simeq 2.2 \times 10^6$ W/cm², where γ is the line width, dominated by the transit-time broadening of 241.5 kHz here, k is the wave vector, $A = 1.6 \times 10^{-5}$ s⁻¹ is the Einstein-A coefficient [25], h is the Planck constant. Under the present experimental conditions, the saturation parameter $S = I_{pump}/I_{sat}$ was in the range of 0.003–0.015. Therefore, the saturation absorption signal was very weak, and the influence of the nonlinear distortion during the ring-down process was limited. Special attention was given to environmental control due to water vapour interference in this spectral region. All optical components were enclosed in a dry-air-purged acrylic box.

The experiment employed a custom cryogenic gas cell (Figure 1) similar to our previous design [26], featuring an electrolytically polished vacuum chamber to minimise blackbody radiation and achieve temperatures as low as 12 K. Two silicon diode sensors (Lakeshore DT-670A-CU) were used to measure the cavity temperature. The uncertainty was about 12 mK at 20 K. It should be noted that there was a temperature gradient of about 1 K along the cell axis ($\sim 8\%$ difference in molecular number density along the cell at 12 K). The gradient was stable under experimental temperatures, and the influence on

the line profile is limited. This cryogenic environment provided two key advantages: it enhanced the population of HD molecules in the $\nu = 0, J = 0$ state by two orders of magnitude compared to room temperature, and reduced pressure-broadened linewidths to the point where transit-time effects dominated, resulting in both stronger signals and improved spectral resolution. The pressure of HD gas in the cavity was determined from the integrated intensity of the Doppler-broadened absorption line, and the uncertainty was estimated to be less than 5%.

3. Result and discussion

The hyperfine splitting and corresponding transition strengths are essential for a precise determination of the transition frequency in the HD molecule due to its complex spectral line shape [16,18]. The rovibrational transitions of HD are complicated by the coupling with the nuclear spin angular momentum of both the proton ($I_H = 1/2$) and the deuteron ($I_D = 1$). Although the HD R(1) (2-0) transition appears stronger than the R(0) line at room temperature, it consists of 21 hyperfine components, as reported in references [27–29]. In contrast, the R(0) transition comprises only 9 transitions, corresponding to five distinct frequency values, resulting in a comparatively simpler spectral structure. The hyperfine splitting of the upper rovibrational level of R(0) spans approximately ± 150 kHz. Figure 2(a) presents the hyperfine-resolved energy level diagram of the HD R(0) (2-0) transition. The upper panel (red curve) of Figure 2(b) displays the simulated R(0) spectrum, where each hyperfine component is modelled with a linewidth of 241 kHz (full width at half maximum, FWHM), corresponding to transit-time broadening [31] at 12 K. No crossover resonances are included in this simulation. The center-of-gravity transition frequency is taken as 214 905 335 320 kHz, based on the latest theoretical value reported by Komasa *et al.* [30] The lower panel shows the measured Lamb-dip spectrum obtained in this work at 12 K and approximately 0.004 Pa, a pressure at which the pressure-broadened linewidth is 5 kHz [18], making further linewidth reduction negligible. Spectral scans were conducted with 40 points per spectrum, each requiring 1 second of data acquisition (0.2 s for stabilisation and 0.8 s for ring-down measurement). Averaging 800 scans over 10 hours yielded a smallest detectable absorption coefficient of 3.5×10^{-13} cm⁻¹.

Figure 3(a,b) show the saturated absorption spectrum of R(0) measured at 12–20 K under various pressures and intra-cavity laser powers. A spectral span of about 2.5 MHz around the Doppler absorption centre

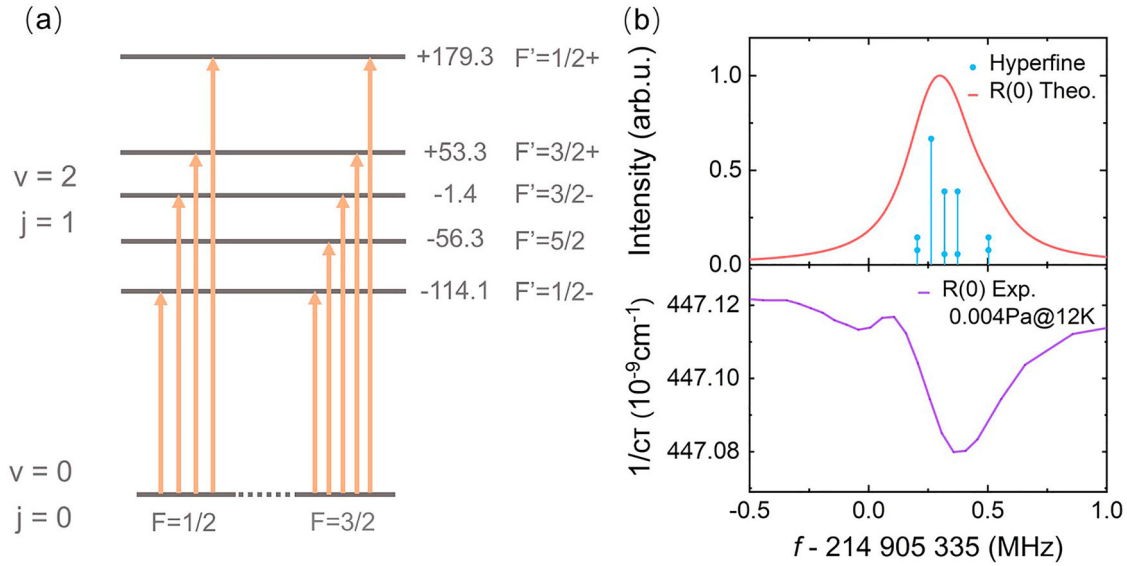


Figure 2. (a) The hyperfine structure [27] of the R(0) (2-0) transition of HD. (b) Upper panel: the simulated spectrum of R(0), as a convolution by a Lorentzian profile with full width at half maximum of 241 kHz of hyperfine lines. The weighted centre is 214 905 335.32 MHz, as given by Komasa *et al.* [30] Blue lines indicate the positions and relative intensities of the hyperfine components [27]. Lower panel: the experimental saturated absorption spectrum measured with the intra-cavity circulating laser power of 200 W, and the baseline is located at $444.4 \times 10^{-9} \text{ cm}^{-1}$.

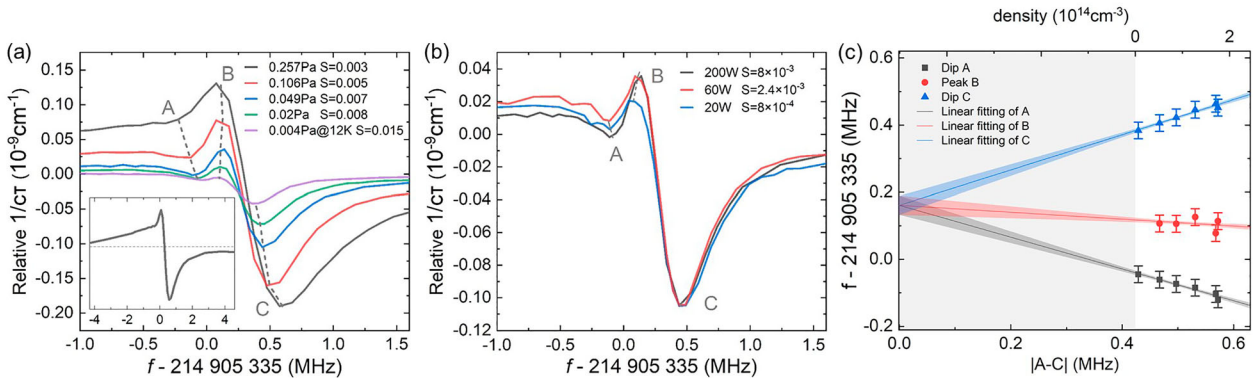


Figure 3. Saturated absorption spectra obtained after subtracting the Doppler-broadened linear absorption background (denoted as ‘Relative $1/c\tau'$ ’). (a) Different sample pressures with the intra-cavity circulating laser power of 200 W at 12–20 K. The inset shows the spectrum in a wider range observed at the pressure ($P \sim 0.257$ Pa). (b) Spectra obtained at different laser powers with a sample pressure of 0.049 Pa at 20 K, normalised by the intra-cavity power. (c) Centre frequency obtained by the ‘lineshape centroid extrapolation’ approach. $|A - C|$: The difference between the frequencies of dips A and C in each spectrum.

was recorded. For clarity, the baselines of the spectra have been vertically offset in the figure. The spectrum reveals unconventional interference patterns and dispersion-like features that differ from conventional Lamb dips. Several characteristic peaks and dips, with positions marked by dashed lines, appear in positions that were not observed in our previous measurements [21] at 76 K. Given that the observed linewidth substantially exceeds the expected hyperfine splitting [27,28], We can confirm that the observed profiles cannot be solely attributed to hyperfine structures. Our measurements, in conjunction with additional data from literature, demonstrate that the asymmetric line profile remains consistently observable across

a pressure range spanning two orders of magnitude (4 mPa to 0.257 Pa) and over a wide temperature interval. Given that collisional effects diminish with decreasing pressure and temperature, these results indicate that collisions are unlikely to be a dominant contributor to the observed line-shape asymmetry.

The pressure-dependent measurements (Figure 3(a)) show systematic shifts in peak/dip positions while maintaining the overall spectral structure. However, dip ‘A’ becomes barely distinguishable at the highest pressure. In contrast, variations in the intra-cavity circulating laser power (Figure 3(b)) predominantly influence the amplitudes of spectral features, which scale approximately

linearly with laser power (or saturation parameter). The positions of these features remain largely unchanged, with only minor intensity variations and slight positional shifts observed in feature ‘B’ at the lowest power (20 W). While the primary spectral feature appears consistent with earlier measurements of the R(1) line [18,21], the newly observed interference patterns constitute an unexpected phenomenon that has not been theoretically predicted [20] and merits further investigation.

To address the challenge of determining the transition frequency from the complex spectral structure, we developed an alternative approach based on characteristic spectral features. Three spectral features labelled ‘A’, ‘B’, and ‘C’ in Figure 3(a,b) were identified from each spectrum. Their positions were determined by identifying local extrema through quadratic spline interpolation followed by numerical differentiation of the spectra. These positions are then plotted as a function of the $|A - C|$ distance, and the corresponding molecular densities are also given in Figure 3(c). As shown in the figure, the three features converge to nearly the same frequency point when the distance is extrapolated to zero. This convergent frequency is taken as the estimated centre of the spectral line. This ‘lineshape centroid extrapolation’ approach, illustrated in Figure 3(c), yielded an intercept frequency of 214 905 335 161 (27)_{stat.} kHz. The robustness of this approach was confirmed through statistical analysis: the exclusion of any individual dataset only influenced the fitting uncertainty, while the extrapolated values remained consistent.

However, two key limitations were identified: (1) the inherent hyperfine structure prevents $|A - C|$ from reaching zero; and (2) the associated systematic uncertainty remains difficult to quantify. It should be noted that the systematic uncertainty is not included in the 27 kHz uncertainty. Here, we provide a quantitative estimate of the uncertainty associated with our lineshape centroid extrapolation method based on several characteristic scales: (1) The half-separation between features ‘A’ and ‘C’ near zero molecular density (Figure 3(c)) is 213 kHz. This value represents an upper bound for the uncertainty. (2) A Lorentzian fit to the theoretically predicted hyperfine structure profile [27,28] yields a half-width of about 124 kHz. (3) The recoil effect is expected to produce a doublet with a splitting of 68 kHz for this specific R(0) (2-0) transition in HD. Given the consistent and well-converging slopes observed for features ‘A’, ‘B’, and ‘C’ in Figure 3(c), we consider the hyperfine-derived width of 124 kHz to be a conservative and representative estimate of the systematic uncertainty introduced by our phenomenological

extraction method. Apart from the systematic uncertainty related to the lineshape centroid extrapolation, other systematic uncertainties can be analysed precisely. Moreover, the collision-induced frequency shift is eliminated in the present method, as shown in Figure 3(c). Other effects, including the frequency comb reference, servo locking stability, and AOM frequency drift, were investigated and found to be negligible in the experiment. We compared the fitted centre frequency obtained from a single-peak Lorentzian model with the center-of-gravity frequency, as shown in the upper panel of Figure 2(b), and derived a correction value of 9 kHz. The second-order Doppler shift is +0.066(3) kHz at 20 K and +0.033(3) kHz at 10 K. After applying the above systematic corrections, the final transition frequency for R(0) is determined to be 214 905 335 170 (27)_{stat} (124)_{sys} kHz. It agrees well with previous experimental results, 214 905 335 220 (20) kHz [12,32] and 214 905 335 240 (100) kHz [33]. The latest theoretical calculations, 214 905 335 320 (450) kHz [30], incorporating optimised high-order relativistic corrections, show excellent agreement with the experimental results.

We do not intend to suggest that the saturation feature should converge to a single frequency at zero width (as distinct from zero pressure). If ultimate resolution were achievable, a set of isolated hyperfine lines would be observed. However, as discussed in this work, reaching such a resolution, whether experimentally or theoretically, appears very challenging at present. The observed ‘converging’ pattern is instead an attempt to approximate the weighted centre of the spectral feature, which may provide useful insight for further analysis. The above approach proves especially valuable in cases where hyperfine structure resolution is infeasible, providing a practical alternative to conventional lineshape fitting methods.

The nonlinear Fano-like resonance (NFR) model [20], which incorporates interactions with far-detuned electronic transitions, successfully reproduces an asymmetric profile characterised by a single ‘peak’ and one ‘dip’ under the highest pressure condition observed in this work. However, since it does not account for hyperfine structure, the model fails to capture the additional ‘dip’ observed at lower pressures. This discrepancy suggests that additional phase differences between perturbing hyperfine states or more physics effects may be taken into account. Although the current theoretical model cannot easily incorporate these effects due to their complexity and the lack of detailed information about electronic-state interactions, the experimental results presented here serve as a benchmark for refining future theoretical models.

4. Conclusions

Our cryogenic saturated absorption spectroscopy of HD at 12 K has revealed intricate spectral asymmetries and complex structures that contradict to the conventional line-shape models. Through centroid extrapolation analysis, we determined the R(0) transition frequency to be 214 905 335 170 (27)_{stat} (124)_{sys} kHz, confirming both previous experimental results and the latest theoretical predictions. While this approach provides robust center-of-gravity frequency determination, we identify complex lineshape effects – rather than instrumental limitations – as the barrier to achieving higher precision. The unexpected spectral complexity observed at low temperatures exceeds current theoretical predictions, highlighting the critical need for advanced lineshape models to unlock new levels of precision in molecular hydrogen spectroscopy.

Acknowledgments

The authors acknowledge Dr. Y.R. Sun for discussions.

Data availability statement

All data are available in the manuscript.

Disclosure statement

No potential conflict of interest was reported by the author(s).

Funding

This work was jointly supported by the Chinese Academy of Science Project for Young Scientists in Basic Research [Grant No.YSBR-055], the Quantum Science and Technology-National Science and Technology Major Project [Grant Nos. 2021ZD0303102, 2023ZD0301000], and the National Natural Science Foundation of China [Grant Nos. 22241302, 12393825].

ORCID

C.-F. Cheng  <http://orcid.org/0000-0003-3637-0989>

S.-M. Hu  <http://orcid.org/0000-0002-1565-8468>

References

- [1] K. Pachucki and J. Komasa, *Phys. Rev. A* **83**, 042510 (2011). doi:10.1103/PhysRevA.83.042510
- [2] K. Pachucki and J. Komasa, *Phys. Rev. A* **83**, 032501 (2011). doi:10.1103/PhysRevA.83.032501
- [3] W. Ubachs, W. Vassen, E.J. Salumbides and K.S.E. Eikema, *Ann. Phys.* **525** (7), A113–A115 (2013). doi:10.1002/andp.v525.7
- [4] W. Ubachs, J.C.J. Koelemeij, K.S.E. Eikema and E.J. Salumbides, *J. Mol. Spectrosc.* **320**, 1–12 (2016). doi:10.1016/j.jms.2015.12.003
- [5] L.G. Tao, A.W. Liu, K. Pachucki, J. Komasa, Y.R. Sun, J. Wang and S.M. Hu, *Phys. Rev. Lett.* **120** (15), 153001 (2018). doi:10.1103/PhysRevLett.120.153001
- [6] M. Beyer, N. Hölsch, J. Hussels, C.F. Cheng, E.J. Salumbides, K.S.E. Eikema, W. Ubachs, C. Jungen and F. Merkt, *Phys. Rev. Lett.* **123**, 163002 (2019). doi:10.1103/PhysRevLett.123.163002
- [7] J. Hussels, N. Hölsch, C.F. Cheng, E.J. Salumbides, H.L. Bethlem, K.S.E. Eikema, Ch. Jungen, M. Beyer, F. Merkt and W. Ubachs, *Phys. Rev. A* **105**, 022820 (2022). doi:10.1103/PhysRevA.105.022820
- [8] M. Puchalski, J. Komasa, A. Spyszkiwicz and K. Pachucki, *Phys. Rev. A* **100** (2), 020503 (2019). doi:10.1103/PhysRevA.100.020503
- [9] R.K. Altmann, L.S. Dreissen, E.J. Salumbides, W. Ubachs and K.S.E. Eikema, *Phys. Rev. Lett.* **120**, 043204 (2018). doi:10.1103/PhysRevLett.120.043204
- [10] N. Hölsch, M. Beyer, E.J. Salumbides, K.S.E. Eikema, W. Ubachs, C. Jungen and F. Merkt, *Phys. Rev. Lett.* **122**, 103002 (2019). doi:10.1103/PhysRevLett.122.103002
- [11] D. Sprecher, C. Jungen and F. Merkt, *J. Chem. Phys.* **140**, 104303 (2014). doi:10.1063/1.4866809
- [12] S. Kassi and A. Campargue, *J. Mol. Spectrosc.* **267** (1–2), 36–42 (2011). doi:10.1016/j.jms.2011.02.001
- [13] S. Vasilchenko, D. Mondelain, S. Kassi, P. Cermák, B. Chomet, A. Garnache, S. Denet, V. Lecocq and A. Campargue, *J. Mol. Spectrosc.* **326**, 9–16 (2016). doi:10.1016/j.jms.2016.04.002
- [14] E. Fasci, A. Castrillo, H. Dinesan, T. Gravina, L. Moretti and L. Gianfrani, *Phys. Rev. A* **98** (2), 022516 (2018). doi:10.1103/PhysRevA.98.022516
- [15] F.M.J. Cozijn, P. Dupré, E.J. Salumbides, K.S.E. Eikema and W. Ubachs, *Phys. Rev. Lett.* **120** (15), 153002 (2018). doi:10.1103/PhysRevLett.120.153002
- [16] M.L. Diouf, F.M.J. Cozijn, B. Darquié, E.J. Salumbides and W. Ubachs, *Opt. Lett.* **44** (19), 4733 (2019). doi:10.1364/OL.44.004733
- [17] M.L. Diouf, F.M.J. Cozijn, K.F. Lai, E.J. Salumbides and W. Ubachs, *Phys. Rev. Res.* **2**, 023209 (2020). doi:10.1103/PhysRevResearch.2.023209
- [18] T.P. Hua, R.Y. Sun and S.M. Hu, *Opt. Lett.* **45** (17), 4863–4866 (2020). doi:10.1364/OL.401879
- [19] A. Fast and S.A. Meek, *Phys. Rev. Lett.* **125** (2), 023001 (2020). doi:10.1103/PhysRevLett.125.023001
- [20] Y.N. Lv, A.W. Liu, Y. Tan, C.L. Hu, T.P. Hua, X.B. Zou, Y.R. Sun, C.L. Zou, G.C. Guo and S.M. Hu, *Phys. Rev. Lett.* **129** (16), 163201 (2022). doi:10.1103/PhysRevLett.129.163201
- [21] Q.H. Liu, Y.N. Lv, C.L. Zou, C.F. Cheng and S.M. Hu, *Phys. Rev. A* **106**, 062805 (2022). doi:10.1103/PhysRevA.106.062805
- [22] F.M.J. Cozijn, M.L. Diouf, W. Ubachs, V. Hermann and M. Schlösser, *Phys. Rev. Lett.* **132**, 113002 (2024). doi:10.1103/PhysRevLett.132.113002
- [23] J. Ye, L.S. Ma and J.L. Hall, *J. Opt. Soc. Am. B* **15** (1), 6–15 (1998). doi:10.1364/JOSAB.15.000006
- [24] G. Giusfredi, S. Bartalini, S. Borri, P. Cancio, I. Galli, D. Mazzotti and P.D. Natale, *Phys. Rev. Lett.* **104**, 110801 (2010). doi:10.1103/PhysRevLett.104.110801
- [25] I.E. Gordon, L.S. Rothman, C. Hill, R.V. Kochanov, Y. Tan, P.F. Bernath, M. Birk, V. Boudon, A. Campargue, K.V. Chance, B.J. Drouin, J.M. Flaud, R.R. Gamache, J.T. Hodges, D. Jacquemart, V.I. Perevalov, A. Perrin,

- K.P. Shine, M.A.H. Smith, J. Tennyson, G.C. Toon, H. Tran, V.G. Tyuterev, A. Barbe, A.G. Császár, V.M. Devi, T. Furtenbacher, J.J. Harrison, J.M. Hartmann, A. Jolly, T.J. Johnson, T. Karman, I. Kleiner, A.A. Kyuberis, J. Loos, O.M. Lyulin, S.T. Massie, S.N. Mikhailenko, N. Moazzen-Ahmadi, H.S.P. Müller, O.V. Naumenko, A.V. Nikitin, O.L. Polyansky, M. Rey, M. Rotger, S.W. Sharpe, K. Sung, E. Starikova, S.A. Tashkun, J.V. Auwera, G. Wagner, J. Wilzewski, P. Wcisło, S. Yu and E.J. Zak, *J. Quant. Spectrosc. Radiat. Transfer* **203**, 3–69 (2017). doi:[10.1016/j.jqsrt.2017.06.038](https://doi.org/10.1016/j.jqsrt.2017.06.038)
- [26] H. Wu, N. Stolarczyk, Q.H. Liu, C.F. Cheng, T.P. Hua, Y.R. Sun and S.M. Hu, *Opt. Express* **27**, 37559 (2019). doi:[10.1364/OE.376572](https://doi.org/10.1364/OE.376572)
- [27] J. Komasa, M. Puchalski and K. Pachucki, *Phys. Rev. A* **102**, 012814 (2020). doi:[10.1103/PhysRevA.102.012814](https://doi.org/10.1103/PhysRevA.102.012814)
- [28] H. Jóźwiak, H. Cybulski and P. Wcisło, *J. Quant. Spectrosc. Radiat. Transf.* **253**, 107171 (2020). doi:[10.1016/j.jqsrt.2020.107171](https://doi.org/10.1016/j.jqsrt.2020.107171)
- [29] P. Dupré, *Phys. Rev. A* **101**, 022504 (2020). doi:[10.1103/PhysRevA.101.022504](https://doi.org/10.1103/PhysRevA.101.022504)
- [30] J. Komasa, *Phys. Rev. A* **113**, 012802 (2026). doi:[10.1103/physrev.113.012802](https://doi.org/10.1103/physrev.113.012802)
- [31] W. Demtröder, *Laser Spectroscopy: Basic Concepts and Instrumentation*, 3rd ed. Springer, Kaiserslautern, Germany (2008).
- [32] S. Kassi, C. Lauzin, J. Chaillot and A. Campargue, *Phys. Chem. Chem. Phys.* **24** (38), 23164–23172 (2022). doi:[10.1039/D2CP02151J](https://doi.org/10.1039/D2CP02151J)
- [33] F.M.J. Cozijn, M.L. Diouf and W. Ubachs, *Euro. Phys. J. D* **76** (11), 220 (2022). doi:[10.1140/epjd/s10053-022-00552-x](https://doi.org/10.1140/epjd/s10053-022-00552-x)